High Order Solution to Exterior 3D Wave Equation by the Method of Difference Potentials

Fouché Frantz Smith, Semyon Tsynkov, and Eli Turkel

1 Introduction

Consider the acoustic wave equation

$$\partial_t^2 u - c^2(\mathbf{x})\Delta u = F(\mathbf{x}, t), \quad (\mathbf{x}, t) \in \mathbb{R}^3 \times (0, T] \tag{1}$$

with zero initial data and a source compactly supported in space. We assume there exists a bounded connected set Υ such that $c(\mathbf{x}) = c_\infty > 0$ whenever $\mathbf{x} \notin \Upsilon$. To solve (1) numerically, we truncate the unbounded domain $\mathbb{R}^3$ with a spherical artificial outer boundary and set a pth order artificial boundary condition (ABC):

$$\partial_t^2 u - c^2(\mathbf{x})\Delta u = F(\mathbf{x}, t), \quad (\mathbf{x}, t) \in \Omega \times (0, T] \tag{2a}$$

$$B_p u = 0 \text{ on } \Gamma \times (0, T] \tag{2b}$$

where $\Omega = \{\mathbf{x} \mid \|\mathbf{x}\|_2 \leq R\}$ such that $\Omega \supset \overline{\Upsilon \cup \text{supp}(F)}$ and $\Gamma = \partial\Omega$. As p increases, the ABC (2b) is expected to better approximate (1). The specific form of the ABC (2b) will be introduced later (see Sect. 3).

F. F. Smith (✉) · S. Tsynkov
Department of Mathematics, North Carolina State University, Raleigh, NC, USA
e-mail: ffsmith@ncsu.edu; tsynkov@math.ncsu.edu

E. Turkel
School of Mathematical Sciences, Tel-Aviv University, Tel Aviv, Israel
e-mail: turkel@tauex.tau.ac.il

© The Author(s), under exclusive license to Springer Nature Switzerland AG 2023

J. M. Melenk et al. (eds.), *Spectral and High Order Methods for Partial Differential Equations ICOSAHOM 2020+1*, Lecture Notes in Computational Science and Engineering 137, https://doi.org/10.1007/978-3-031-20432-6_30

2 Fourth Order Compact Scheme (FOCS)

We construct a fourth order discretization of the exterior acoustic wave equation using a $3 \times 3 \times 3$ stencil in space and three levels in time. Given the uniform time step τ, applying the θ-scheme [9] to (1) produces a one parameter family of EPDEs on the upper time level

$$(\Delta - \kappa^2)u^{n+1} = f^{n+1} \triangleq \left(2 - {}^1\!/\!_\theta\right) f^n - f^{n-1} - \kappa^2 u^n/\theta - \left(F^{n+1} + ({}^1\!/\!_\theta - 2)F^n + F^{n-1}\right)/c^2 \tag{3}$$

where $\kappa^2 = (\theta\tau^2 c^2(\mathbf{x}))^{-1}$. When $\theta = {}^1\!/\!_{12}$, (3) is fourth order accurate in t. Applying an "equation based" compact finite difference scheme[1] to (3) yields a fourth order compact scheme (FOCS)

$$\mathbf{L}_h[\kappa^2]u^{n+1}_{i,j,k} = h^2 f^{n+1}_{\mathbf{R}} \triangleq h^2 \mathbf{R}_h f^{n+1}_{i,j,k} = h^2 \left(2f^{n+1}_{i,j,k}/3 + f^{n+1}_{ss}/36 + f^{n+1}_{sc}/72\right). \tag{4}$$

The LHS operator in (4) is given by

$$\mathbf{L}_h[\kappa^2]u_{i,j,k} \triangleq -4u_{i,j,k} + u_{ss}/3 + u_{sc}/6 - h^2 \left(2(\kappa^2 u)_{i,j,k}/3 + (\kappa^2 u)_{ss}/36 + (\kappa^2 u)_{sc}/72\right)$$

where $u_{ss} = \sum_{\substack{-1 \le \bar{i},\bar{j},\bar{k} \le 1 \\ |\bar{i}|+|\bar{j}|+|\bar{k}|=1}} u_{i+\bar{i},j+\bar{j},k+\bar{k}}$ and $u_{sc} = \sum_{\substack{-1 \le \bar{i},\bar{j},\bar{k} \le 1 \\ |\bar{i}|+|\bar{j}|+|\bar{k}|=2}} u_{i+\bar{i},j+\bar{j},k+\bar{k}}$. The CFL number, $\lambda(\mathbf{x}) = c(\mathbf{x})\tau/h$ should satisfy $\max_{\mathbf{x}} \lambda(\mathbf{x}) \le \sqrt{5/8}$ to guarantee stability. For a complete derivation of the FOCS, the CFL number, and numerical validation over a cubic domain see our previous results in [21].

3 Method of Difference Potentials (MDP)

We apply the θ-scheme (Sect. 2) to the truncated problem (2) and choose the radiation boundary condition [7] for (2b). This ABC introduces new artificial variables v_j on the outer artificial boundary. We then define a sequence of equations (one for each v_j) along the outer boundary. The number of v_j determines the accuracy of the ABC as a function of the size (diameter) of Ω. Thus, problem (2) becomes

$$(\Delta - \kappa^2)u^{n+1} = f^{n+1}, \quad \mathbf{x} \in \Omega \tag{5a}$$

$$({}^{\partial_t}\!/\!_{c_\infty} + \partial_r + {}^1\!/\!_R)u^{n+1} = v_1^{n+1}, \quad \mathbf{x} \in \Gamma \tag{5b}$$

$$\left({}^{\partial_t}\!/\!_{c_\infty} + {}^j\!/\!_R\right)v_j^{n+1} = ({}^{j(j-1)+\Delta_{\theta,\varphi}})v_{j-1}^{n+1}/4R^2 + v_{j+1}^{n+1}, \ \mathbf{x} \in \Gamma, \ j = 1, \ldots, p \tag{5c}$$

[1] Start with a central difference formula including the leading error term. Second, differentiate the governing equation to replace the high order derivatives contained in the leading error term. Third, approximate this expression with central differences. See [21] for detail.

where $v_0^{n+1} = 2u^{n+1}$ and $v_{p+1}^{n+1} = 0$. We refer to (5b)–(5c) as NRBC(p). We chose this ABC because it works in spherical geometry where we have formulated the elliptic PDE and it is easy to implement for any given p. Note that in [11], we used a different approach and defined the high order BGT ABCs (time harmonic case) directly.

Advancing the time marching scheme amounts to solving the EPDE (5) at every time step. The method of difference potentials (MDP) utilizes the uniformly discretized FOCS, but has the capacity to handle the curvilinear geometry of Ω. Difference potentials can be considered discrete counterparts to Calderon-Seeley potentials which reduce a given PDE to an equivalent pseudo-differential equation on the boundary of its domain. The MDP embeds the BVP (5) into a simple cubic auxiliary domain $\Omega^0 \supset \Omega$ while the Calderon-Seeley potentials are approximated with difference potentials constructed from the discrete solution operator to the EPDE on the auxiliary domain. Since the equation is positive definite and the auxiliary domain is a cube, a geometric multigrid method can compute the discrete solution operator in $O(N \log N)$ operations and achieve optimal (multigrid) convergence rates [22]. In addition, the MDP uses a spectral representation of the boundary condition on Γ. See the monograph [18] for more on the MDP and [1, 3–6, 10, 14, 19] for various applications of the MDP.

In Sect. 3.1, we define some constructs pertinent to the MDP. In Sect. 3.2, we introduce the Boundary Equation with Projection (BEP) and the governing theorem which shows the relationship between the solution to the BEP and the solution to (5) on Ω. In Sect. 3.3, we show how to solve the BEP.

3.1 Preliminaries

The following constructs are necessary to solve the EPDE (5) at every time step.

- **Grid Sets**: Let $\mathbb{N}^0/\mathbb{M}^0$ denote the uniform mesh of Ω^0 including/excluding the boundary nodes, $\Gamma^0 = \mathbb{N}^0 \setminus \mathbb{M}^0$, $\mathbb{M}^+ = \mathbb{M}^0 \cap \bar{\Omega}$, and $\mathbb{M}^- = \mathbb{M}^0 \setminus \mathbb{M}^+$. For any $(x_i, y_j, z_k) \in \mathbb{M}^0$, let $\mathcal{N}_{i,j,k} = \{(x_{i+\bar{i}}, y_{j+\bar{j}}, z_{k+\bar{k}}) \mid |\bar{i}|, |\bar{j}|, |\bar{k}| \leq 1,\ \ 1 \leq |\bar{i}| + |\bar{j}| + |\bar{k}| \leq 2\}$. Then let $\mathbb{N}^{\pm} = \{\cup \mathcal{N}_{i,j,k} \mid (x_i, y_j, z_k) \in \mathbb{M}^{\pm}\}$. Finally, the discrete boundary $\gamma = \mathbb{N}^+ \cap \mathbb{N}^-$ are nodes which straddle the continuous boundary Γ. Choose Ω^0 large enough so $\gamma \cap \Gamma^0 = \emptyset$.
- **Auxiliary Problem (AP):** Given the discrete AP $\mathbf{L}_h[\kappa^2]w = g$ in $\mathbb{M}^0$ and $w = 0$ on Γ^0, where the RHS g on $\mathbb{M}^0$ can be arbitrary, the *solution operator* $\mathbf{G}_h$ (Green's operator) produces the unique solution $w = \mathbf{G}_h g$ to the discrete AP.
- **Difference Potential:** A *density*, v_γ, is a grid function supported on γ. The *difference potential* with density v_γ is $v_{\mathbb{N}^+} = \mathbf{P}_{\mathbb{N}^+} v_\gamma = w - \mathbf{G}_h\big(\mathbf{L}_h[\kappa^2]w|_{\mathbb{M}^+}\big)$, where $v_\gamma = w|_\gamma$ and the *difference projection* is $\mathbf{P}_\gamma v_\gamma = \mathbf{P}_{\mathbb{N}^+} v_\gamma|_\gamma$.

3.2 Boundary Equation with Projection (BEP)

The following theorem (Theorem 1.1.7 [18] or Proposition 3.4 [23]) gives us a representation of the solution to the BVP (5) using the difference potential.

Theorem 1 (Boundary Equations of Calderón-Seely Type) *Consider the discrete EPDE*

$$\mathbf{L}_h[\kappa^2]u^{n+1}_{\mathbb{N}^+} = h^2\,\tilde{f}^{n+1}_{\mathbf{R}} = \begin{cases} 0, & \mathbf{x}_h \in \mathbb{M}^- \\ h^2 f^{n+1}_{\mathbf{R}}, & \mathbf{x}_h \in \mathbb{M}^+ \end{cases} \tag{6}$$

where the RHS is assembled according to (3). The density u^{n+1}_{γ} coincides with the trace of a solution to (6) on γ: $u^{n+1}_{\gamma} = u^{n+1}_{\mathbb{N}^+}|_{\gamma}$, if and only if it satisfies the inhomogeneous BEP

$$u^{n+1}_{\gamma} = \mathbf{P}_{\gamma} u^{n+1}_{\gamma} + \mathbf{G}_h \tilde{f}^{n+1}_{\mathbf{R}}|_{\gamma}. \tag{7}$$

If the above holds, $u^{n+1}_{\mathbb{N}^+}$ is given by the generalized Green's formula:

$$u^{n+1}_{\mathbb{N}^+} = \mathbf{P}_{\mathbb{N}^+} u^{n+1}_{\gamma} + \mathbf{G}_h \tilde{f}^{n+1}_{\mathbf{R}}|_{\mathbb{N}^+}. \tag{8}$$

Note that Theorem 1 doesn't make any explicit reference to the boundary condition on Γ. It shows how the trace of the solution, $u^{n+1}_{\gamma} = u^{n+1}_{\mathbb{N}^+}|_{\Gamma}$, can be substituted into the generalized Green's Formula (8) to solve the discrete EPDE (6). However, the boundary condition on Γ is necessary to construct u^{n+1}_{γ}.

3.3 Solving the Boundary Equation with Projection

The density u^{n+1}_{γ} is obtained from $\boldsymbol{\xi}^{n+1}_{\Gamma} = \left(u^{n+1}|_{\Gamma}, \partial_r u^{n+1}|_{\Gamma}\right)$ by applying an affine operator called the extension operator (see Appendix 1). It is derived using a combination of Taylor's Theorem about the continuous boundary Γ and a spectral representation of $\boldsymbol{\xi}^{n+1}_{\Gamma}$ in terms of spherical harmonics (recall, Ω is a sphere). From Theorem 1, the trace of the discrete solution must satisfy the inhomogeneous BEP (7). Consequently, substituting (21) into (7) yields the linear system

$$\mathbf{Q}_0\mathbf{c}^{n+1}_0 + \mathbf{Q}_1\mathbf{c}^{n+1}_1 = -\mathbf{G}_h \tilde{f}^{n+1}_{\mathbf{R}}|_{\mathbb{N}^+} - \mathbf{q}^{n+1}_I. \tag{9}$$

$\mathbf{Q}_i \in \mathbb{C}^{|\gamma|\times(1+L)^2}$ in (9) is the result of applying $\mathbf{P}_{\gamma} - \mathbf{I}_{\gamma}$ to each of the columns of $\mathbf{A}_i \in \mathbb{C}^{|\gamma|\times(1+L)^2}$ (defined in (21), Appendix 1), $\mathbf{q}^{n+1}_I = (\mathbf{P}_{\gamma} - \mathbf{I}_{\gamma})\mathbf{E}\mathbf{x}^{n+1}_I$ ($\mathbf{E}\mathbf{x}^{n+1}_I$ defined in (18)), and $\mathbf{c}^{n+1}_i \in \mathbb{C}^{(1+L)^2}$ (defined in (22)) are the Fourier coefficients of $\partial^i_r u^{n+1}|_{\Gamma}$. $\mathbf{Q}_0$ and $\mathbf{Q}_1$ require $(1+L)^2$ calls of the solution operator $\mathbf{G}_h$. However,

$\mathbf{P}_{\mathbb{N}^+}(\alpha_{lm}^{(i)} Y_l^m) = (-1)^m \mathbf{P}_{\mathbb{N}^+}(\alpha_{lm}^{(i)} Y_l^m)^*$ [14, Eq. (53)] reduces the number of times we need to call $\mathbf{G}_h$ by nearly one half. The matrices $\mathbf{Q}_0$ and $\mathbf{Q}_1$ only need to be computed once as they don't depend on time. Since we assume the solution to the exterior problem (1) is smooth[2] the total number of columns $(1+L)^2 \ll |\gamma|$. The spectral form of NRBC(p) provides the additional equations necessary to solve for both unknowns in (9). Accordingly, (5b)–(5c) satisfies (see [7, eqs. (40) and (45)])

$$(\partial_t/c_\infty + \partial_r + 1/R)u = \sum_{l=1}^{\infty} \sum_{m=-l}^{l} (\mathbf{v}_{lm} \cdot \mathbf{e}_1) Y_l^m(\theta, \varphi)$$

$$\mathrm{d}\mathbf{v}_{lm}/\mathrm{d}t = \mathbf{A}_l \mathbf{v}_{lm} - l(l+1)c_\infty \langle u, Y_l^m \rangle \mathbf{e}_1/2R^2$$

where $\mathbf{v}_{lm} = [v_{lm}^{(1)}, \ldots, v_{lm}^{(p)}]^T \in \mathbb{C}^p$, $\mathbf{e}_1 = [1, 0, \ldots, 0]^T \in \mathbb{R}^p$, the tridiagonal matrix $\mathbf{A}_l$ contains $-\frac{c_\infty}{R}[1, \ldots, p]^T \in \mathbb{R}^p$ along the diagonal, $c_\infty[1, \ldots, 1]^T \in \mathbb{R}^{p-1}$ along the superdiagonal, and $\frac{c_\infty}{4R^2}[2(1) - l(l+1), \ldots, p(p-1) - l(l+1)]^T \in \mathbb{R}^{p-1}$ along the subdiagonal, and the weighted inner product is defined in (19). We truncate the auxiliary variables of NRBC(p) using $l = 0, \ldots, L$ and $m = -l, \ldots, l$ to be consistent with the truncation of the extension operator (see Appendix 1). First, we discretize the spectral boundary condition in time. If we discretize the ODE $\mathrm{d}w/\mathrm{d}t = g$ with the fourth order linear multistep method backwards differentiation formula (BDF4) $w^{n+1} + \sum_{j=1}^{4} a_j w^{n+1-j} = b_0 \tau g^{n+1}$ [15], replace u and $\partial_r u$ with the expansion (20), use orthogonality of the spherical harmonics (19), and combine like terms, we obtain a system of equations for the Fourier coefficients:

$$-\sum_{j=1}^{4} a_i \left\langle u^{n+1-j}, Y_0^0 \right\rangle = (1 + \tau c_\infty b_0/R) \left\langle u^{n+1}, Y_0^0 \right\rangle + \tau c_\infty b_0 \left\langle \partial_r u, Y_0^0 \right\rangle \quad (10a)$$

$$-\sum_{j=1}^{4} a_i \mathbf{\Phi}_{lm}^{n+1-j} = \hat{\mathbf{A}}_l \mathbf{\Phi}_{lm}^{n+1} + \left\langle \partial_r u^{n+1}, Y_l^m \right\rangle \mathbf{b}_l, \; l = 1, \ldots, L, \; |m| \le l, \quad (10b)$$

$\mathbf{\Phi}_{lm} = [\langle u, Y_l^m \rangle, \mathbf{v}_{lm}]^T \in \mathbb{C}^{p+1}$, $\mathbf{b}_l = [\tau c_\infty b_0, 0, \ldots, 0]^T \in \mathbb{R}^{p+1}$, and the tridiagonal matrix

$$\hat{\mathbf{A}}_l = \left(\begin{array}{c|c} (1 + \tau c_\infty b_0/R) & -\tau b_0 c_\infty \mathbf{e}_1^T \\ \hline \tau b_0 l(l+1) c_\infty \mathbf{e}_1/2R^2 & \mathbf{I}_{p \times p} - \tau b_0 \mathbf{A}_l \end{array} \right) \in \mathbb{R}^{p+1 \times p+1} \quad (11)$$

[2] Let $g \in C^{k,\gamma}(\mathbb{S}^2)$ for some $k \ge 0$ and $\gamma \in (0, 1]$ such that $k + \gamma > 1/2$. Then there exists $C > 0$ such that $\|g - \mathscr{Q}_L g\|_\infty \le C/L^{k+\gamma-1/2}$ where $\mathscr{Q}_L g$ is the orthogonal projection of g on the space of polynomials of degree $\le L$ on $\mathbb{S}^2$ [2, Corollary 4.14].

Rearranging (10) yields:

$$-\sum_{j=1}^{4} \frac{a_i}{1+\tau c_\infty b_0/R} \langle u^{n+1-j}, Y_0^0 \rangle = \left\langle u^{n+1}, Y_0^0 \right\rangle + \frac{\tau c_\infty b_0}{1+\tau c_\infty b_0/R} \langle \partial_r u^{n+1}, Y_0^0 \rangle \tag{12a}$$

$$-\hat{\mathbf{A}}_l^{-1} \left(\sum_{j=1}^{4} a_i \mathbf{\Phi}_{lm}^{n+1-j} \right) = \mathbf{\Phi}_{lm}^{n+1} + \langle \partial_r u^{n+1}, Y_l^m \rangle \hat{\mathbf{A}}_l^{-1} \mathbf{b}_l, l = 1, \ldots, L, |m| \leq l. \tag{12b}$$

Now we are in a position to substitute the spectral form of NRBC(p) into (9). Since (9) doesn't depend on the auxiliary variables $\mathbf{v}_{lm}^{n+1}$ we extract the equations in (12) which only include the Fourier coefficients of $(u^{n+1}|_\Gamma, \partial_r u^{n+1}|_\Gamma)$. If we take the first component of (12b) for $l = 1, \ldots, L$ and $m = -l, \ldots, l$ along with (12a) and arrange them as a linear system where the lm-th component is placed in row $l(l+1)+m+1$, then

$$\mathbf{c}_0^{n+1} + \mathbf{M}\mathbf{c}_1^{n+1} = \mathbf{c}_{\mathrm{NRBC}(p)}^{n+1} \tag{13}$$

where

$$\mathbf{M} = \mathrm{diag}\left(\frac{\tau c_\infty b_0}{1+\tau c_\infty b_0/R}, \hat{\mathbf{A}}_1^{-1} \mathbf{b}_1 \cdot \tilde{\mathbf{e}}_1, \ldots, \hat{\mathbf{A}}_L^{-1} \mathbf{b}_L \cdot \tilde{\mathbf{e}}_1 \right)$$

and

$$\mathbf{c}_{\mathrm{NRBC}(p)}^{n+1} = -\sum_{j=1}^{4} a_j \left(\frac{\langle u^{n+1-j}, Y_0^0 \rangle}{1+\tau c_\infty b_0/R}, \hat{\mathbf{A}}_1^{-1} \mathbf{\Phi}_{1,-1}^{n+1-j} \cdot \tilde{\mathbf{e}}_1, \ldots, \hat{\mathbf{A}}_L^{-1} \mathbf{\Phi}_{L,L}^{n+1-j} \cdot \tilde{\mathbf{e}}_1 \right)^T$$

and $\tilde{\mathbf{e}}_1 = [1, 0, \ldots, 0]^T \in \mathbb{R}^{p+1}$. Substituting (13) into (9) yields:

$$\left(\mathbf{Q}_1 - \mathbf{Q}_0\mathbf{M}\right)\mathbf{c}_1 = -\mathbf{Q}_0 \mathbf{c}_{\mathrm{NRBC}(p)}^{n+1} - \mathbf{G}_h \tilde{f}_{\mathbf{R}}^{n+1}|_{\mathbb{N}^+} - \mathbf{q}_I^{n+1}. \tag{14}$$

The overdetermined system (14) is solved for $\boldsymbol{c}_1^{n+1}$ in the sense of least squares using QR factorization. Then $\boldsymbol{c}_0^{n+1}$ is computed with (13). The NRBC(p) auxiliary variables $\mathbf{v}_{lm}^{n+1}$ are computed from (12b) for $l = 1, \ldots, L$ and $m = -l, \ldots, l$. Now that the Fourier coefficients are all known we can use the extension operator (21) to compute the density u_γ^{n+1} which we substitute into the generalized Green's formula (8) to compute the solution $u_{\mathbb{N}^+}^{n+1}$ and advance the time marching scheme.

4 Numerical Simulations

Table 1 defines the components of our test problems (see Appendix 2). For **T1**, the direction of propagation is normal to Γ which corresponds to the maximum absorption. For **T2**, the off-center location of the center of the source implies the solution no longer meets Γ at a right angle. For **T3**, the off center location of the source and differentiation defined by means of the multi-index $\boldsymbol{\alpha}$ generate even more asymmetry than **T2**. In addition, the source term provides continuous output for all $t > 0$. Finally, **T4** and **T5** repeat **T1** and **T2** respectively with variable speed. In all our simulations $R = 1.5$, $\Omega^0 = [-2, 2]^3$, $L = 18$, and the termination criteria is $\|r_h^{(i)}\| \leq 10^{-12}\|r_h^{(0)}\| + 10^{-12}$ where the residual of the ith iteration is $r_h^{(i)} = g - \boldsymbol{L}_h u_h^{(i)}$. For our multigrid method we use the V(1,1) cycle per iteration using full-weighting as the restriction operator and tri-cubic interpolation as the prolongation operator.

Figure 1 qualitatively demonstrates why high order ABCs are necessary. A grid refinement analysis would fail to demonstrate fourth order accuracy since the plots from several grids overlap when $t \in (4, 5)$. Increasing the order of the NRBC clearly improves the absorption since the gap between dash and dashed-dotted (or dashed-dotted and dotted) plots increases over the interval when $t \in (4, 5)$. However, the order isn't high enough to eliminate the reflection error on each and every grid.

To perform a full-fledged grid refinement analysis we run our simulations with NRBC(6). Table 2 shows fourth order convergence for all test problems defined in Table 1. Recall that, there are two sources of error. The first source of error is the reflection error due to replacing (1) with (2), which decreases as the order of NRBC(p) increases. The second source of error is the discretization error from the FOCS which decreases as the grid is refined. An ABC of a sufficiently high order guarantees the reflection errors are so much smaller than the discretization error that refining the grid effectively produces fourth order convergence. There exists a sufficiently fine grid where refining the grid no longer improves the overall error as seen Fig. 1. Fortunately, a high order ABC decreases the "floor" of this threshold value.

Table 1 Components of the Test solution and source term defined in Appendix 2

Name	$\boldsymbol{\alpha}$	R_0	m	$\mathbf{x}_0$	t_0	$S(t)$	c^2
T1	(0, 0, 0)	1.5	7	(0, 0, 0)	3.0	$5(1 - 12t^2)\exp(-6t^2)$	1
T2	(0, 0, 0)	1.0	7	$(15/100, 15/100, 15/100)$	4.0	$\sin(8t)\exp(-6t^2)$	1
T3	(1, 1, 0)	0.75	12	$(0, 0, 1/4)$	0.2	$\left(\sin^{11}(\pi t/5) + \frac{1}{\sqrt{3}}\sin^{11}(\pi t/5\sqrt{2})\right)\chi_{(0,\infty)}$	1
T4	(0, 0, 0)	1.5	7	(0, 0, 0)	3.0	$5(1 - 12t^2)\exp(-6t^2)$	$4/5 + \exp(-20\|\mathbf{x}\|_2^2)/5$
T5	(0, 0, 0)	1.0	7	$(15/100, 15/100, 15/100)$	4.0	$\sin(8t)\exp(-6t^2)$	$4/5 + \exp(-20\|\mathbf{x}\|_2^2)/5$

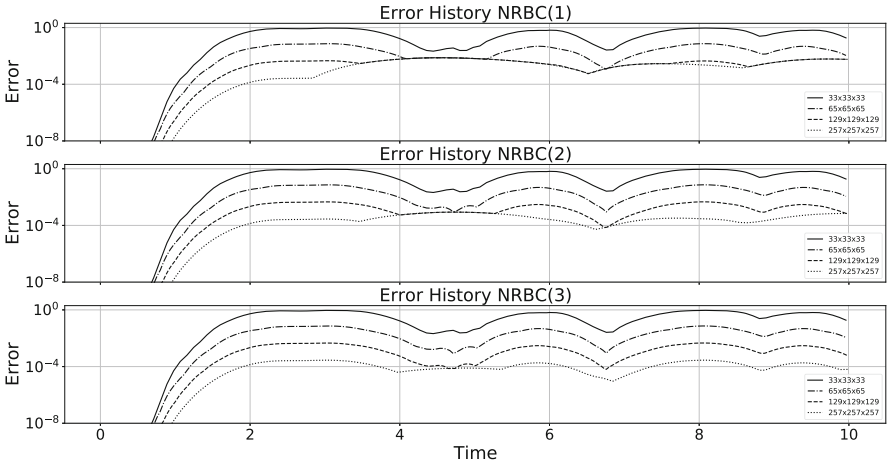

Fig. 1 Error history for **T3** for low order NRBC with respect to the infinity norm

Table 2 Error (∞-norm on $\mathbb{M}^+$) when using NRBC(6), $\tau = {}^{9h}\sqrt{5/8}/10$, and $T = 10.0$

				CPUTIME (s)		Avg. # multigrid iterations		
	h	Error	Rate	get $\mathbf{Q}_0, \mathbf{Q}_1$	Time marching	$\mathbf{G}_h \tilde{f}_{\mathbf{R}}^{n+1}$	$\mathbf{q}_I^{n+1}$	$\mathbf{P}_{\mathbb{N}^+} u_\gamma^{n+1}$
T1	4/33	9.55e-01	–	10.1	56.7	4.28	3.96	3.96
	4/65	3.75e-02	4.67	138.7	916.2	4.09	3.71	3.66
	4/129	2.24e-03	4.07	1328.7	12984.4	3.69	3.41	3.37
	4/257	1.37e-04	4.03	10524.03	195352.92	3.41	3.20	3.11
T2	4/33	7.92e-01	–	9.9	25.1	3.79	3.53	3.52
	4/65	5.10e-02	3.96	135.0	393.9	3.73	3.38	3.25
	4/129	2.73e-03	4.22	1343.9	5720.4	3.38	3.13	3.06
	4/257	1.55e-04	4.05	10572.62	79376.43	3.18	3.02	2.88
T3	4/33	9.33e-01	–	10.1	23.0	4.64	4.36	4.39
	4/65	7.34e-02	3.67	140.1	392.1	4.64	4.31	4.32
	4/129	4.61e-03	3.99	1346.2	5577.1	4.64	4.29	4.29
	4/257	2.84e-04	4.02	10514.64	80684.77	4.63	4.29	4.28
T4	4/33	1.85e+01	–	10.8	26.78	4.96	4.49	4.35
	4/65	7.09e-02	4.71	165.37	431.53	4.54	4.14	4.03
	4/129	3.84e-03	4.21	1571.36	6266.19	4.40	3.97	3.80
	4/257	2.31e-04	4.06	11931.39	90038.02	4.02	3.73	3.59
T5	4/33	1.10e+00	–	10.78	17.28	4.13	3.98	3.73
	4/65	1.06e-01	3.38	161.66	260.71	4.02	3.71	3.55
	4/129	4.90e-03	4.43	1454.40	3439.12	3.95	3.50	3.37
	4/257	2.87e-04	4.09	11821.86	49433.50	3.60	3.36	3.22

5 Concluding Remarks and Future Work

We derived a high order scheme for (1) using a combination of the θ-scheme, a compact finite difference scheme in space, multigrid, the MDP, and a high order ABC. Our numerical examples demonstrate that if the order of the ABC is *sufficiently* high, refining the grid *effectively* produces fourth order accuracy.

A perfectly matched layer (PML) is another approach to truncating unbounded problems. A PML is a layer surrounding the domain which rapidly attenuates any incoming waves. Modern PMLs are derived by transforming the governing equation in time to the frequency space, using a complex coordinate transformation, performing some algebraic manipulation, and transforming back to the time space. The PML modified governing equation resembles the original governing equation with some additional parameters and some auxiliary equations supported in the PML. Discretizing PMLs with high order accuracy while maintaining long term stability is challenging. Instead, we derived a FOCS for a Cartesian sponge layer [8], which behaves similarly to a PML without the additional auxiliary equations, but offers less effective absorption. We were able to demonstrate fourth order convergence provided the sponge layer was sufficiently thick. Otherwise the convergence rate would stall. This mirrors the results shown in Sect. 4.

In the future, we will solve the three dimensional wave scattering problem about a spherical body adapting the current high order MDP scheme as a foundation. We will close the unbounded problem with NRBC(p) or the newly developed sponge layer [8], construct an auxiliary problem which contains the scattering region and the above closure, then define a similar BEP to solve the scattering problem.

Appendix 1: Extension Operator

Consider the pair $\left(\mathbf{x}_h, \tilde{\mathbf{x}}_h\right) \in (\gamma, \Gamma)$ where $\tilde{\mathbf{x}}_h$ is the orthogonal projection of $\mathbf{x}_h$ onto Γ. By Taylor's Theorem

$$\mathbf{Ex}(\boldsymbol{\xi}^{n+1}) = \left(u^{n+1} + \varrho\partial_r u^{n+1} + \sum_{j=2}^{4} \frac{\varrho^j}{j!}\partial_r^j u^{n+1}\right)|_{\tilde{\boldsymbol{x}}_h} + O(\varrho^5) \tag{15}$$

where $\varrho = |\mathbf{x}_h - \tilde{\mathbf{x}}_h|$ if $\mathbf{x}_h \notin \Omega$ or $\varrho = -|\mathbf{x}_h - \tilde{\mathbf{x}}_h|$ if $\mathbf{x}_h \in \Omega$. We choose a fifth order extension operator even though we only desire fourth order accuracy. According to Reznik's Theorem [16, 17], a sixth order extension operator is sufficient for maintaining fourth order accuracy for a second order PDE discretized with fourth order accuracy. However, Reznik's Theorem isn't always necessary. For example, [3] uses a fourth order MDP scheme for the 2D acoustic wave equation using a fourth order extension operator. Dirichlet boundary conditions maintained fourth order accuracy, but Neumann boundary conditions dropped to third order accuracy. Thus, we opted for a fifth order accurate extension operator. Differentiating the acoustic wave equation (1) in spherical coordinates (i.e. $\Delta u = \partial_r^2 u + \frac{2}{r}\partial_r u + {}^{\Delta_{\theta,\varphi}u}/r^2$)

yields the high order derivatives:

$$\partial_r^2 u = -\left((2/R)\partial_r u + \Delta_{\theta,\varphi} u/R^2\right) + (1/c_\infty^2)\partial_t^2 u \tag{16a}$$

$$\partial_r^3 u = \partial_t^2 \partial_r u/c_\infty^2 - 2\partial_t^2 u/(c_\infty^2 R) + (6-\Delta_{\theta,\varphi})\partial_r u/R^2 + 4\Delta_{\theta,\varphi} u/R^3 \tag{16b}$$

$$\partial_r^4 u = (8-\Delta_{\theta,\varphi})\partial_t^2 u/(c_\infty^2 R^2) - 2\partial_t^2 \partial_r u/(c_\infty^2 R) + \partial_t^2 \partial_r^2 u/c_\infty^2 + (\Delta_{\theta,\varphi}^2 - 18\Delta_{\theta,\varphi})u/R^4 + (8\Delta_{\theta,\varphi} - 24)\partial_r u/R^3 \tag{16c}$$

since the source term is zero on Γ and the speed $c(\boldsymbol{x}) = c_\infty$ on Γ. Replacing the time derivatives of (16) with the one sided difference scheme in time $\partial_r^i \partial_t^2 u^{n+1} = d_i^{n+1} \partial_r^i u^{n+1} + \sum_{j=0}^{n_i} d_i^{n-j} \partial_r^i u^{n-j} + O(\tau^{n_i})$, which preserves fifth order accuracy since $\tau = O(\varrho)$, and substituting the expressions into (15) leads to

$$\begin{aligned}\mathbf{Ex}(\boldsymbol{\xi}^{n+1}) = {} & \Big[1 + \varrho^2\Big(d_0^{n+1}/c_\infty^2 - \Delta_{\theta,\varphi}/R^2\Big)/2 + \varrho^3\Big(-2d_0^{n+1}/(c_\infty^2 R) + 4\Delta_{\theta,\varphi}/R^3\Big)/6 + \varrho^4\Big(d_0^{n+1} d_2^{n+1}/c_\infty^4 \\ & + (\Delta_{\theta,\varphi}^2 - 18\Delta_{\theta,\varphi})/R^4 + (8d_0^{n+1} - (d_0^{n+1} + d_2^{n+1})\Delta_{\theta,\varphi})/(c_\infty^2 R^2)\Big)/24\Big] u^{n+1} + \Big[\varrho - \varrho^2/R \\ & + \varrho^3\Big((6-\Delta_{\theta,\varphi})/R^2 + d_1^{n+1}/c_\infty^2\Big)/6 - \varrho^4\Big(2(d_2^{n+1} + d_1^{n+1})/(c_\infty^2 R) + (24 - 8\Delta_{\theta,\varphi})/R^3\Big)/24\Big]\partial_r u^{n+1} + \mathbf{Ex}_I^{n+1}\end{aligned} \tag{17}$$

where the inhomogeneous term is given by

$$\begin{aligned}\mathbf{Ex}_I^{n+1} = {} & \Big[\varrho^2/(2c_\infty^2) - \varrho^3/(3c_\infty^2 R) + \varrho^4\Big((8-\Delta_{\theta,\varphi})/(c_\infty^2 R^2) + d_2^{n+1}/c_\infty^4\Big)/24\Big] \sum_{j=0}^{n_0} d_0^{n-j} u^{n-j} \\ & + \Big[\varrho^3/(6c_\infty^2) - \varrho^4/(12c_\infty^2 R)\Big] \sum_{j=0}^{n_1} d_1^{n-j} \partial_r u^{n-j} + (\varrho^4/(24c_\infty^2)) \sum_{j=0}^{n_2} d_2^{n-j} \partial_r^2 u^{n-j}.\end{aligned} \tag{18}$$

Finally, we introduce the spectral form of the trace $\boldsymbol{\xi}_\Gamma^{n+1} = (u^{n+1}|_\Gamma, \partial_r u^{n+1}|_\Gamma)$ using spherical harmonics as our basis functions. The spherical harmonics are eigenfunctions of the Laplace-Beltrami operator, i.e., $\Delta_{\theta,\varphi} Y_l^m(\theta,\varphi) = -l(l+1)Y_l^m(\theta,\varphi)$ on the unit sphere $\mathbb{S}^2$ [2, Section 3.3] and form an orthonormal basis on the sphere of radius R centered at the origin with respect to the weighted inner product [2, eq. (4.6)]:

$$\langle v, w\rangle = \int_0^{2\pi} \int_0^{\pi} v(R,\theta,\varphi) w(R,\theta,\varphi)^* \sin(\theta) \mathrm{d}\theta \mathrm{d}\varphi \tag{19}$$

The derivatives are given by

$$\partial_r^k u \approx \sum_{l=0}^{L} \sum_{m=-l}^{l} \left\langle \partial_r^k u, Y_l^m \right\rangle Y_l^m(\theta,\varphi), \quad \text{on } \Gamma, \quad k = 0, 1, \ldots \tag{20}$$

and then the extension operator (17) becomes

$$u_\gamma^{n+1} = \mathbf{Ex}(\boldsymbol{\xi}^{n+1}) = \boldsymbol{A}_0\mathbf{c}_0^{n+1} + \boldsymbol{A}_1\mathbf{c}_1^{n+1} + \mathbf{Ex}_I^{n+1} \tag{21}$$

The matrices are given by

$$\mathbf{A}_i = \left[\alpha_{0,0}^{(i)} Y_0^0 \;\; \alpha_{1,-1}^{(i)} Y_1^{-1} \;\; \alpha_{1,0}^{(i)} Y_1^0 \;\; \alpha_{1,1}^{(i)} Y_1^1 \;\; \ldots \;\; \alpha_{L,L}^{(i)} Y_L^L\right], \quad i \in \{0, 1\}$$

where the coefficients are

$$\begin{aligned}
\alpha_{lm}^{(0)} &= 1 + \varrho^2\left(d_0^{n+1}/c_\infty^2 + l(l+1)/R^2\right)/2 - \varrho^3\left(2d_0^{n+1}/(c_\infty^2 R) + 4l(l+1)/R^3\right)/6 \\
&\quad + \varrho^4\left(l(l+1)(l(l+1)+18)/R^4 + d_0^{n+1}d_2^{n+1}/c_\infty^4 + (8d_0^{n+1} + (d_0^{n+1} + d_2^{n+1})l(l+1))/(c_\infty^2 R^2)\right)/24 \\
\alpha_{lm}^{(1)} &= \varrho - \varrho^2/R + \varrho^3\left((6 + l(l+1))/R^2 + d_1^{n+1}/c_\infty^2\right)/6 - \varrho^4\left(2(d_2^{n+1} + d_1^{n+1})/(c_\infty^2 R) + (8l(l+1)+24)/R^3\right)/24
\end{aligned}$$

and the Fourier coefficients are

$$\boldsymbol{c}_i^n = \left[\langle \partial_r^i u^n, Y_0^0 \rangle \;\; \langle \partial_r^i u^n, Y_1^{-1} \rangle \;\; \ldots \;\; \langle \partial_r^i u^n, Y_L^L \rangle\right]^T, \quad i \in \{0, 1, 2\} \tag{22}$$

Substituting the expansions (20) into (18) produces the spectral from of $\mathbf{Ex}_I^{n+1}$. To compute the spherical harmonics numerically, see [12]. Given $g \in C(\mathbb{S})$, the Fourier coefficients $\langle g, Y_l^m \rangle$ for $l = 0, 1, \ldots, L$ and $m = -l, \ldots, l$ can be computed fast using the spherical harmonic transform described in [20].

Appendix 2: Generating Test Solutions

The function

$$u(\mathbf{x}, t) = S(t - t_0 - r/c)/(4\pi r) \quad \text{with} \quad r = \|\mathbf{x} - \mathbf{x}_0\|_2 \tag{23}$$

solves the wave equation (1), with constant speed c, driven by the point source term $F(\mathbf{x}, t) = \delta_{\mathbf{x}_0}(\mathbf{x})S(t)$. We construct a family of smooth test solutions similar to (23) employing the same strategy as [13, Section 8.2]. Define the test solution

$$u^{\text{Test}}(\mathbf{x}, t) = D^{\boldsymbol{\alpha}}\left(\phi_m(r/R_0)S(t - t_0 - r/c)/(4\pi r)\right) \tag{24}$$

where $D^{\boldsymbol{\alpha}} = \partial^{|\boldsymbol{\alpha}|}/\partial x^{\alpha_1}\partial y^{\alpha_2}\partial z^{\alpha_3}$, and the smooth step function is defined as follows

$$\phi_m(r) = \begin{cases} r^{m+1}\sum_{k=0}^m \binom{m+k}{m}\binom{2m+1}{m-k}(-r)^k & \text{if } 0 \le r < 1 \\ 1 & \text{if } r \ge 1 \end{cases}$$

Since $\phi_m(r/R_0)/r = O(r^m)$ as $r \downarrow 0$, (24) vanishes at $\mathbf{x}_0$ provided $m > |\boldsymbol{\alpha}|$. By construction, (24) equals (23) on the complement of the sphere of radius R_0 centered at $\mathbf{x}_0$ when $|\boldsymbol{\alpha}| = 0$, and satisfies the acoustic wave equation (1) where the source term is given by

$$F^{\text{Test}}(\mathbf{x}, t) \triangleq D^{\boldsymbol{\alpha}}\left(c\phi_m'(r/R_0)S'(t-t_0-r/c)/(2\pi R_0 r) - c^2\phi_m''(r/R_0)S(t-t_0-r/c)/(4\pi R_0^2 r)\right) \tag{25}$$

The source term (25) is compactly supported in space in the ball of radius R_0 centered at $\mathbf{x}_0$. The translation t_0 is chosen sufficiently large so that the initial data are zero (up to machine precision) assuming that S is a smooth rapidly decaying function or compactly supported.

To generate a family of test solutions with variable speed, consider a function of the form $\phi_m(r/R_0)S(t-t_0-r/c(\mathbf{x}))/(4\pi r)$, then follow the same procedure as outlined above. The resulting source term will be supported on the union of Υ and the sphere of radius R_0 centered at $\mathbf{x}_0$.

Acknowledgments Work supported by the US Army Research Office (ARO) under grant W911NF-16-1-0115 and the US–Israel Binational Science Foundation (BSF) under grants 2014048 and 2020128.

References

1. Albright, J., Epshteyn, Y., Steffen, K.R.: High-order accurate difference potentials methods for parabolic problems. Appl. Numer. Math. **93**, 87–106 (2015)
2. Atkinson, K., Han, W.: Spherical Harmonics and Approximations on the Unit Sphere: An Introduction. Lecture Notes in Mathematics. Springer Berlin Heidelberg, Berlin, Heidelberg (2012)
3. Britt, S., Tsynkov, S., Turkel, E.: Numerical solution of the wave equation with variable wave speed on nonconforming domains by high-order difference potentials. J. Comput. Phys. **354**, 26–42 (2018)
4. Epshteyn, Y.: Upwind-difference potentials method for Patlak-Keller-Segel chemotaxis model. J. Sci. Comput. **53**(3), 689–713 (2012)
5. Epshteyn, Y., Xia, Q.: Efficient numerical algorithms based on difference potentials for chemotaxis systems in 3d. J. Sci. Comput. **80**(1), 26–59 (2019)
6. Epshteyn, Y., Xia, Q.: Difference potentials method for models with dynamic boundary conditions and bulk-surface problems. Adv. Comput. Math. **46**(5), 1–39 (2020)
7. Huan, R., Thompson, L.L.: Accurate radiation boundary conditions for the time-dependent wave equation on unbounded domains. Int. J. Numer. Methods Eng. **47**(9), 1569–1603 (2000). https://doi.org/10.1002/(SICI)1097-0207(20000330)47:9<1569::AID-NME845>3.0.CO;2-9
8. Kahana, A., Smith, F., Turkel, E., Tsynkov, S.: A high order compact time/space finite difference scheme for the 2D and 3D wave equation with a damping layer. J. Comput. Phys. **460**, Paper No. 111161 (2022)
9. Liang, H., Liu, M.Z., Lv, W.: Stability of θ-schemes in the numerical solution of a partial differential equation with piecewise continuous arguments. Appl. Math. Lett. **23**(2), 198–206 (2010)

10. Medvinsky, M., Tsynkov, S., Turkel, E.: The method of difference potentials for the Helmholtz equation using compact high order schemes. J. Sci. Comput. **53**(1), 150–193 (2012)
11. Medvinsky, M., Tsynkov, S., Turkel, E.: Direct implementation of high order BGT artificial boundary conditions. J. Comput. Phys. **376**, 98–128 (2019)
12. Mohlenkamp, M.J.: A user's guide to spherical harmonics (2010)
13. Petropavlovsky, S., Tsynkov, S.: Non-deteriorating time domain numerical algorithms for Maxwell's electrodynamics. J. Comput. Phys. **336**, 1–35 (2017)
14. Petropavlovsky, S., Tsynkov, S., Turkel, E.: A method of boundary equations for unsteady hyperbolic problems in 3d. J. Comput. Phys. **365**, 294–323 (2018)
15. Ralston, A., Rabinowitz, P.: A First Course in Numerical Analysis. Courier Corporation (2001)
16. Reznik, A.A.: Approximation of surface potentials of elliptic operators by difference potentials. Soviet Math. Dokl. **25**(2), 543–545 (1982)
17. Reznik, A.A.: Approximation of the surface potentials of elliptic operators by difference potentials and solution of boundary-value problems. Ph.D. thesis, Moscow Institute for Physics and Technology, Moscow, USSR (1983). [in Russian]
18. Ryaben'kii, V.S.: Method of Difference Potentials and Its Applications, Springer Series in Computational Mathematics, vol. 30. Springer, Berlin (2002)
19. Ryaben'kii, V., Torgashov, V.: An iteration-free approach to solving the navier–stokes equations by implicit finite difference schemes in the vorticity-stream function formulation. J. Sci. Comput. **81**(3), 1136–1149 (2019)
20. Schaeffer, N.: Efficient spherical harmonic transforms aimed at pseudospectral numerical simulations. Geochem. Geophys. Geosyst. **14**(3), 751–758 (2013)
21. Smith, F., Tsynkov, S., Turkel, E.: Compact high order accurate schemes for the three dimensional wave equation. J. Sci. Comput. **81**(3), 1181–1209 (2019)
22. Trottenberg, U., Schuller, A.: Multigrid. Academic Press, Orlando (2001)
23. Utyuzhnikov, S.V.: Generalized Calderón-Ryaben'kii's potentials. IMA J. Appl. Math. **74**(1), 128–148 (2009)